Fin performance with condensation from humid air: a numerical investigation

J. E. R. Coney and C. G. W. Sheppard
University of Leeds, Department of Mechanical Engineering, Leeds, UK

E. A. M. El-Shafei
Mansoura University, Department of Mechanical and Power Engineering, Mansoura, Egypt

The performance of cooling coils in air conditioning equipment is affected by condensation, which may form on the fins of the coil tubing. Extending well established theories, a numerical method has been evolved for condensation from a humid air flow. Considering a cooled vertical fin, a heat and mass transfer analogy is applied to the conjugation of convected heat and mass in a buffer layer, adjacent to the condensate layer, with heat conduction through the fin. The fin temperature distribution, the condensate film thickness and the fin effectiveness are predicted, numerically, for a fin in a laminar humid air cross flow. The variations in these values show that condensation has a substantial influence on fin performance, the reduction in fin effectiveness being a function of the additional heat associated with latent heat when condensation occurs.

Keywords: condensation; dehumidification; numerical methods

Introduction

In the past, the performance of dehumidifying coils, used in air conditioning plants, has been analyzed in a number of ways. Goodman[1,2] used an analogy between heat and mass transfer, based on the assumption that the Lewis number of humid air is unity and that the relationship between the temperature and the enthalpy of saturated air is linear. Tuve *et al.*[3] studied the performance of dehumidying coils assuming that the relative humidity of the air, as it passes through the coils, is virtually constant. However, this method is applicable only to the dehumidification of saturated air.

Threlkeld[4] investigated fin performance with respect to dehumidification and modified the conventional one-dimensional fin analysis; in particular, he assumed the fin to be covered with a uniform condensate film. The air Conditioning and Refrigeration Institute, in their standard 410-72,[5] presented a now widely accepted method for estimated wet finned coil performance, an adaptation of that of Ware and Hacha.[6] Although this method gives good results for design and rating purposes, it has undesirable features; e.g., the coil surface temperature is assumed to be the only parameter affecting the fin effectiveness, regardless of the moist air conditions. With condensation on the fin surface, it was stated in Ref. 5 that the fin efficiency was constant and less than that of the dry fin by 12%, regardless of the upstream moist air conditions.

McQuiston[7] analyzed the performance of a fin of uniform cross section, which took into account the effect of mass transfer from the humid air. An energy balance on an elemental volume was made, assuming one-dimensional heat transfer and the process line between the inlet and exit conditions on the psychrometric chart to be straight. He derived a differential equation describing the fin temperature distribution. From this solution, it was found that the fin efficiency decreased because of the presence of condensation and with increasing air relative humidity. At high relative humidities, the results of Ref. 7 agreed with those of Ref. 5, indicating that the latter is sufficiently accurate for design and performance calculations.

Kilic and Onat[8] analyzed the performance of a vertical rectangular fin with dehumidification of air. Both heat and mass transfer coefficients along the vertical height of the fin were taken as constant. Equating the conductive heat transfer through the fin with the sum of convective heat and latent heat of condensation from the surrounding humid air, they found that, for a given parameter ($m=\sqrt{2h_{ad}k_f t}$), the fin temperature increased as the transverse fin length increased. Also, the rate of condensation decreased and the ratio of heat transfers in the wet and dry cases was a maximum at $mL=0.80$. On the other hand, the fin effectiveness with condensation was less than that for the dry case.

The present theoretical approach, based on the studies presented in Ref. 9, extends these methods, making them more comprehensively applicable to the study of the performance of fins in dehumidification processes. In particular, more precise psychrometric data has been incorporated than in the previous studies. Also, a wide range of airflow parameters (velocity, relative humidity, dry-bulb temperature) and fin base temperatures are considered.

Theoretical analysis

In dehumidification processes, heat and mass transfer occur from the saturated air layer to the condensate film with latent heat transfer to the fin. The effect of subcooling has also been investigated by others.[10] Since the energy associated with the subcooling of the condensate layer has been shown to be very small compared with that liberated as latent heat during condensation of vapor, it is ignored in the present study.

A theoretical analysis for a laminar condensate film formed in the presence of a laminar airflow, is therefore presented.

Address reprint requests to Dr. Coney at the University of Leeds, Department of Mechanical Engineering, Leeds LS2 9JT, UK.

Received 25 August 1987; accepted 21 November 1988

Assumptions

The following assumptions are made to reduce the real problem to one more readily soluble.

(1) Temperature variations across both the fin thickness and its width are small and may be neglected.
(2) The thermal conductivity of the fin material is constant.
(3) Heat transfer from the end and the edges of the fin may be neglected.
(4) The temperature at each point on the fin surface is below the dew point of the bulk humid air.
(5) The humid airflow is steady and one-dimensional.
(6) The local air-side heat transfer and mass transfer coefficients are constant.
(7) The condensate forms a smooth continuous film on the fin surface and flows under the effect of gravity only. The condensate film is assumed thin relative to the test section dimensions, such that it does not affect the humid airflow. Conversely, the effect of shear on the condensate film is ignored.
(8) The inertia and convective forces within the condensate film have a negligible effect on the heat transfer coefficient.
(9) The effect of small amplitude condensate waves, if existing, on the condensate heat transfer coefficient is insignificant.
(10) All properties of the condensate are constant and are determined at the mean fin temperature.
(11) The liquid–vapor and the liquid–wall interfacial thermal resistances are negligible.
(12) The air–vapor mixture (humid air) is assumed to be well mixed such that concentration gradients in the bulk are zero.

The condensation process on the fin

A vertical flat fin of thickness t, width L, height H, and having thermal conductivity k_f, is considered. At its upper edge, it is cooled and maintained at a constant temperature, T_{fb}. A thin layer of condensate collects on the fin surface next to which is a film of air–vapor mixture, where the concentration of vapor is lower than in the bulk humid air. Due to the partial pressure gradient of the water vapor in the thin air–vapor film, vapor diffuses from the main body of the flow through that film and liquifies at the condensate–humid air interface. This transfer augments the condensate layer on the fin surface.

The physical model and coordinate system are shown in Figure 1. From the assumptions listed both the condensate film thickness δ_c and the fin temperature T_f vary transversely to the airflow (i.e., in the x-direction) and their distributions depend on the humid air conditions (ϕ_∞, T_∞, V_∞). At $x=0$, $T_f=T_{fb}$ and the condensation rate is a maximum.

Under the action of gravity, the condensate flows down the fin, its thickness growing with x. Hence, the thermal resistance of the condensate increases, thereby decreasing both the condensation and the heat transfer rates.

Notation

A	Parameter in Equation 11
B	Parameter in Equation 11
C	Variable defined by Equation 9
c_{p_a}	Specific heat of dry air, J/kg K
c_{p_c}	Specific heat of condensate, J/kg K
D	Parameter in Equation 11
g	Acceleration due to gravity, m/s^2
h_c	Condensate heat transfer coefficient, W/m^2 K
$\bar{h}_c$	Average condensate heat transfer coefficient, W/m^2 K
h_{ad}	Heat transfer coefficient (dry air–solid interface), W/m^2 K
h_m	Mass transfer coefficient, m/s
h_{ov}	Overall air heat transfer coefficient W/m^2 K
H	Fin height, m
k_c	Condensate thermal conductivity, W/m K
k_f	Fin material thermal conductivity, W/m K
L	Longitudinal fin length, m
$\dot{m}_c$	Condensate mass flux, kg/m^2 s
N	Dimensionless parameter, defined by Equation 32
$\dot{q}$	Local heat flux at the interface between the air–vapor and the condensate films, W/m^2
$\dot{q}_{id}$	Local heat flux
q_f	Local heat flux at the fin surface, W/m^2
$\dot{q}_L$	Rate of latent heat liberated per unit area, W/m^2
$\dot{q}_s$	Rate of sensible heat transfer per unit area, W/m^2
Q_f	Overall rate of heat transfer, W
Q_{idf}	Overall rate of heat transfer for an ideal (isothermal) fin, W
R	Dimensionless parameter
t	Fin thickness, m
T_i	Interfacial temperature, K
T_f	Fin temperature, K
T_{fb}	Fin base temperature, K
T_{fx}	Local fin temperature, K
T_∞	Bulk air temperature, K
V_x	Velocity in condensate film due to gravity, m/s
V_∞	Bulk air velocity, m/s
x	Vertical coordinate
X	Dimensionless coordinate, defined by Equation 25
y	Coordinate normal to the fin surface
z	Longitudinal (streamwise) coordinate

Greek symbols

γ_c	Specific weight of the condensate, N/m^3
δ_c	Condensate film thickness, m
δ_H	Thickness of equivalent laminar film for heat transfer, m
δ_M	Thickness of equivalent laminar film for mass transfer, m
Δ	Dimensionless film thickness, defined by Equation 25
ν	Kinematic viscosity, m^2/s
θ	Dimensionless fin temperature, defined by Equation 11
θ'	Dimensionless temperature gradient, dθ/dx
$(\theta')_0$	Dimensionless temperature gradient at fin base
λ	Latent heat of evaporation, J/kg
ρ_a	Dry air density, kg/m^3
ρ_c	Condensate density, kg/m^3
ϕ_∞	Bulk air relative humidity
n_w	Wet fin effectiveness
ω_f	Moisture content of saturated air at T_f, kg$_w$/kg$_a$
ω_i	Moisture content of saturated air at T_i, kg$_w$/kg$_a$
ω_∞	Bulk air moisture content, kg$_w$/kg$_a$
dT/dx	Temperature gradient in x-direction, K/m

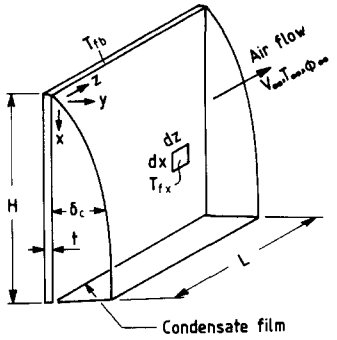

Figure 1 The physical model and coordinate system

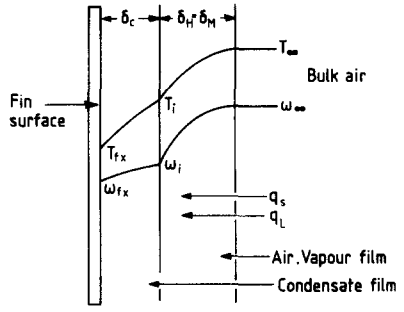

Figure 2 Temperature and concentration profiles in the humid air film and condensate film

Model formulation

Physical model and coordinate system. For the fin, an energy balance for a volumetric element $(t, \mathrm{d}x, \mathrm{d}z)$ at x, z (Figure 1) involves conductive heat flows within the fin in the x-direction and an inflow of heat from the condensate, and by convection from the bulk humid air.

For condensation on both sides of the fin, it is given by

$$-k_f(t\ \mathrm{d}z)\frac{\mathrm{d}^2T_{fx}}{\mathrm{d}x^2}=\dot{q}_{fx}(2\ \mathrm{d}x\ \mathrm{d}z) \tag{1}$$

Simultaneous heat and mass transfer from the humid air to the condensate film. Because of the presence of concentration and temperature gradients in the air–vapor film adjacent to the condensate film, both mass and energy will be transferred through that film to the condensing surface, as shown in Figure 2.

The heat flux $\dot{q}$ from the bulk humid air to the condensation film comprises two parts:

(i) convective heat transfer, $\dot{q}_s$, due to the temperature gradient,
(ii) heat liberated at the interface due to condensation, $\dot{q}_L$.

Hence,

$$\dot{q}=\dot{q}_s+\dot{q}_L \tag{2}$$

The mass transfer coefficient is thus defined

$$\dot{m}_c=\rho_a h_m(\omega_\infty-\omega_i) \tag{3}$$

Now, the water vapor condensed on the fin must be supplied with its latent heat of condensation λ. Hence, the resultant heat flux at the interface is

$$\dot{q}_L=\rho_a h_m\lambda(\omega_\infty-\omega_i) \tag{4}$$

Since the Lewis number for air and water vapor mixture is near unity, Equation 4 may be written as

$$\dot{q}_L=\frac{h_{ad}\lambda}{c_{p_a}}(\omega_\infty-\omega_i) \tag{5}$$

Also since the effect of mass transfer on the gas-phase heat transfer coefficient is negligible, the condensation rate being low

$$\dot{q}_s=h_{ad}(T_\infty-T_i) \tag{6}$$

Thus, from Equations 2, 5, and 6

$$\dot{q}=h_{ad}(T_\infty-T_i)\left[1+\frac{\lambda}{c_{p_a}}\left(\frac{\omega_\infty-\omega_i}{T_\infty-T_i}\right)\right] \tag{7}$$

Equation 7 is nonlinear in T_i, the major nonlinearity arising because ω_i depends on the interface temperature T_i. If $\omega_\infty-\omega_i$ is related to $T_\infty-T_i$, $\dot{q}$ can be assumed as a function of T_i only,

$$q=h_{ad}(T_\infty-T_i)\left[1+\frac{\lambda C}{c_{p_a}}\right] \tag{8}$$

where

$$C=\frac{\omega_\infty-\omega_i}{T_\infty-T_i}\cong\frac{\omega_\infty-\omega_{fx}}{T_\infty-T_{fx}} \tag{9}$$

if the assumption is made that $T_i=T_{fx}$, the condensate film being very thin.

Now a second-degree polynomial relationship fits the psychrometric chart saturation line sufficiently well in the region of the fin temperature variation.

Therefore from Equation 11

$$\omega_f=1.2075-0.9125\times10^{-2}T_{fx}+0.1726\times10^{-4}T_{fx}^2 \tag{10}$$

From Equations 10 and 9,

$$C=\frac{A+B\theta-D\theta^2}{\theta} \tag{11}$$

where

$$A=\frac{\omega_\infty-1.2075+0.9125\times10^{-2}T_{fx}-0.1726\times10^{-4}T_\infty^2}{T_\infty-T_{fb}}$$

$$B=0.3452\times10^{-4}T_\infty-0.9125\times10^{-2}$$

$$D=0.1726\times10^{-4}(T_\infty-T_{fb})$$

$\theta=\dfrac{T_\infty-T_{fx}}{T_\infty-T_{fb}}$, the dimensionless temperature

Overall heat transfer coefficient. During the condensation of vapor from humid air, the total amount of heat liberated, as given by Equation 8, may be described by an overall air heat transfer coefficient which accounts for both sensible heat and that due to condensation. Thus

$$\dot{q}=h_{ov}(T_\infty-T_i) \tag{12}$$

where

$$h_{ov}=\left[1+\frac{\lambda C}{c_{p_a}}\right]h_{ad} \tag{13}$$

It is accepted that a temperature difference occurs at the condensate–humid air interface. However, since this interface is only 1–2 molecules thick, its thermal resistance will be very low; and the interfacial temperature difference negligible.

Hence considering heat transfer through the condensate film

$$\dot{q}_{fx}=\frac{k_c}{\delta_c}(T_i-T_{fx}) \tag{14}$$

Equation 14 describes the local heat flux at the fin surface

assuming linearity in the temperature profile across the condensate film, in the absence of subcooling.

The effect of a nonlinear temperature profile in the liquid film, where subcooling occurs, has been investigated by Sparrow and Gregg.[12] They found that, because of the thinness of the condensate film, the energy associated with its subcooling is very small compared with that liberated as latent heat during condensation of vapor. Hence, the effect of the Jakob number,

$$\frac{c_{p_a}(T_i - T_{fx})}{\lambda}$$

even for a high value (0.1) as in the normal operating range, adds only some 1.5% to the heat transfer coefficient.

Now, from Equations 1 and 14,

$$\frac{d^2T_{fx}}{dx^2} = \frac{-2k_c}{k_f t \delta_c}(T_i - T_{fx}) \tag{15}$$

and from Equations 12 and 14,

$$T_i = T_{fx} + (T_\infty - T_{fx})\left[\frac{h_{ov}\delta_c}{h_{ov}\delta_c + k_c}\right] \tag{16}$$

Hence, from Equations 15 and 16

$$\frac{d^2T_{fx}}{dx^2} = \frac{-2k_c h_{ov}}{k_f t(h_{ov}\delta_c + k_c)}(T_\infty - T_{fx}) \tag{17}$$

In order to solve Equation 17 to obtain the fin temperature distribution T_{fx} and the condensate film thickness distribution, δ_c, the mass flow of the film and the condensation process producing the flow must be considered.

A laminar condensate film is shown schematically in Figure 3.

Since the flow of such a film is under gravity only, the velocity distribution may be written as

$$V_x = \frac{g}{2\nu_c}(2y\delta_c - y^2) \tag{18}$$

The rate $\dot{m}_c$ at which the condensate passes through an element of area ($\delta_c\, dz$), at position x, z is obtained by integrating Equation 18, giving

$$\dot{m}_{c_x} = \frac{g\rho_c}{3\nu_c}\delta_c^3\, dz \tag{19}$$

The change of $\dot{m}_{c_x}$ in the vertical direction between (x, z) and $(x+\Delta x, z)$ is then

$$d\dot{m}_{c_x} = \frac{\gamma_c}{\nu_c}\delta_c^2\left(\frac{d\delta_c}{dx}\right)dx\, dz \tag{20}$$

This change in $\dot{m}_{c_x}$ is caused by the addition of condensate at the interface. Consequently, the rate at which latent heat is liberated per unit surface area at (x, z) is

$$q_L = \lambda\frac{d\dot{m}_{c_x}}{dx\, dz} = \left[\frac{\gamma_c\lambda}{\nu_c}\delta_c^2\right]\frac{d\delta_c}{dx} \tag{21}$$

Now from Equations 5 and 21

$$T_\infty - T_i = \left[\frac{\gamma_c c_{p_a}}{h_{ad}\nu_c C}\right]\delta_c^2\frac{d\delta_c}{dx} \tag{22}$$

From Equations 16 and 22

$$(h_{ov}\delta_c + k_c)\frac{d\delta_c}{dx} = \frac{k_c\nu_c h_{ad}C}{\gamma_c c_{p_a}}(T_\infty - T_{fx}) \tag{23}$$

The governing equations resulting from this analysis, are Equations 17 and 23. When solved, these equations give both the fin temperature distribution and the condensate film thickness distribution with the transverse direction x.

Boundary conditions

At $x=0$, the fin temperature is at its base value, i.e., $T_{fx} = T_{fb}$, specified constant.

The situation at the fin tip, $x=H$, is complex. For a tip insulated fin, $dT/dx = 0$ at $x=H$. For a fin with an uninsulated tip, this is not true. However, insulation will be assumed since it introduces less error than the approximation $T_f = T_x$ at $x=H$.

Therefore, for the assessment of condensate film thickness and fin temperature, the boundary conditions are

$$\begin{aligned} &T_f(0) = T_{fb} \\ &\frac{dT}{dx}(H) = 0 \\ &\delta_c(0) = 0 \end{aligned} \tag{24}$$

Normalization of the problem

The following normalized variables are introduced:

$$\begin{aligned} &\Delta = \delta_c/H \\ &X = x/H \end{aligned} \tag{25}$$

Using these variables, together with θ, Equations 17 and 23 become, respectively,

$$\frac{d^2\theta}{dx^2} = \frac{S\theta}{\Delta + N} \tag{26}$$

$$\frac{d\Delta}{dX} = \frac{\theta}{J(R\Delta^3 + \Delta^2)} \tag{27}$$

where

$$\begin{aligned} &S = \frac{2k_c H}{k_f t} \\ &N = \frac{1}{R} = \frac{k_c}{h_{ov}H} \\ &J = \frac{\gamma_c c_{p_a} H^2}{h_{ad}\nu_c C(T_\infty - T_{fb})} \end{aligned} \tag{28}$$

By substituting h_{ov} (Equation 13) and C (Equation 11) into

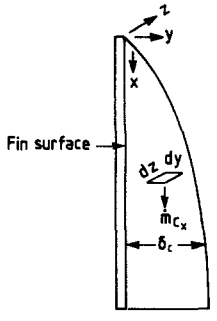

Figure 3 Laminar condensate film

Equation 28, the fin parameters emerge as

$$S=\frac{2k_cH}{k_ft}$$

$$N=\frac{1}{R}=\frac{\theta}{A_1+A_2\theta-A_3\theta^2} \quad (29)$$

$$J=\frac{\gamma_c\lambda H^3\theta}{Z_1(A_1+A_4\theta-A_3\theta^2)}$$

where

$$A_1=Z_2A$$

$$A_2=Z_2B+\frac{h_{ad}H}{k_c}$$

$$A_3=Z_2D$$

$$A_4=Z_2B$$

$$Z_1=k_c\nu_c(T_\infty-T_{fb})$$

$$Z_2=\frac{h_{ad}H}{k_cc_{p_a}}$$

After normalizing the governing equations, the boundary conditions (Equation 28) must be reformulated in terms of the transformed variables. Thus

$$\theta(0)=1.0$$

$$\frac{d\theta}{dX}(1)=0.0 \quad (30)$$

$$\Delta(0)=0.0$$

The normalized quantities. In the formulation of the boundary value problem, described by Equations 26, 27, and 30, several important quantities appeared:

(i) the normalized variables X, θ, and Δ.
(ii) the normalized fin parameters, which have a direct bearing on fin performance in wet operations, as follows:

S: the effect of fin material and geometry.
N: the effect of the surrounding, immersing, fluid.
J: the effect of both previous parameters and also that due to coolant temperature variations.

The following theoretical analysis will take into account:

(a) aluminum as the fin material.
(b) a humid air temperature range of 298 K–323 K.
(c) an air velocity range of 1.0–4.0 m/s.
(d) an air relative humidity range of 50%–100%.
(e) a coolant temperature range of 275 K–285 K.

Fin effectiveness formulation

The significant result from the solution of Equations 17 and 23 is the fin heat transfer rate. At any value of z, the local heat flux from the fin to its base surface is given by Fourier's law, thus

$$\dot{q}_f=-k_f\left[\frac{dT}{dx}\right]_0 \quad (31)$$

or, in terms of the dimensionless variables,

$$\dot{q}_f=\frac{k_f(T_\infty-T_{fb})}{H}\left[-\frac{d\theta}{dX}\right] \quad (32)$$

Hence, the overall rate of heat transfer for the fin over its total depth is

$$\dot{Q}_f=\frac{k_f(T_\infty-T_{fb})}{H}\left(-\frac{d\theta}{dX}\right)\int_0^L t\,dZ \quad (33)$$

i.e.,

$$\dot{Q}_f=k_ft\left(\frac{L}{H}\right)(T_\infty-T_{fb})\left(\frac{d\theta}{dX}\right)_0 \quad (34)$$

The ideal fin. An ideal fin will be considered, the temperature of which, T_f is uniform and equal to the fin base temperature T_{fb}. The temperature at the interface of the condensate and the air–vapor mixture will be assumed uniform also. Since the condensate film thickness is very small, it is assumed that this interface temperature, T_i, is equal to the fin temperature, T_f. Hence, the rate of heat transfer from the moist air to a horizontal strip of fin at x with a surface area ($L\,dx$) is

$$\dot{q}_{id(x)}=2h_{ov}(T_\infty-T_{fb})(L\,dx) \quad (35)$$

The overall rate of heat transfer ($\dot{Q}_{idf}$) from the fin to its base over a vertical height from $x=0$ to $x=H$, is then

$$\dot{Q}_{idf}=2h_{ov}(T_\infty-T_{fb})\int_0^h L\,dx$$

i.e.,

$$\dot{Q}_{idf}=2h_{ov}HL(T_\infty-T_{fb}) \quad (36)$$

From Equations 34 and 36, the fin effectiveness $\dot{q}_f/\dot{q}_{idf}$ is

$$\frac{k_ft(L/H)(T_\infty-T_{fb})}{2h_{ov}HL(T_\infty-T_{fb})}\left[-\frac{d\theta}{dX}\right]_0$$

or

Effectiveness

$$\eta_w=\frac{N}{S}\left[-\frac{d\theta}{dX}\right]_0 \quad (37)$$

Numerical solution of the governing equations

Equations 26, 27, and 30 are complex, involving coupled nonlinear ordinary differential equations. Hence an analytical solution is difficult, and may be replaced by a numerical solution.

Since the problem is of the boundary value type, the subroutine used to solve it had to be incorporated into a search procedure. This produced, for the calculated fin parameter, the appropriate value of $\Delta(0)$ and $\Delta(1)$ for which Equation 30 is satisfied.

The technique, which has been used to solve the present problem, uses an initial value and a Newtonian iteration. (See Appendix.)

Results and discussion

Air dry-bulb temperature

Graphs of computed values of θ, Δ, and θ' against X at various air dry-bulb temperatures are plotted in Figure 4. Figure 4(a) shows that the calculated dimensionless fin temperature decreases with increasing X. With increasing air dry-bulb temperature T_∞, the heat transfer potential becomes higher, causing a reduction in the values of θ. In consequence, the fin temperature at all points increases, due to the enhanced rate of heat transfer from the humid air to the fin surface.

The dimensionless condensate film thickness Δ is plotted

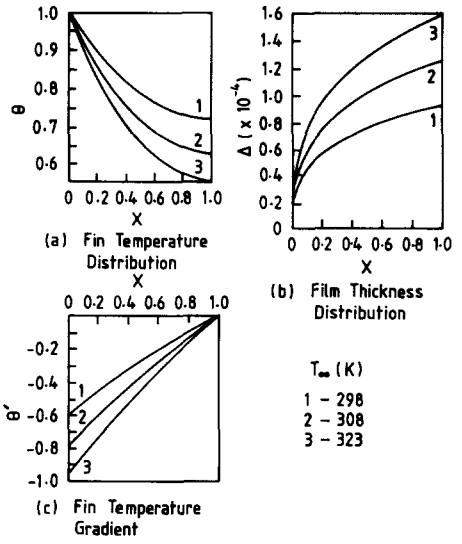

Figure 4 Effect of T_∞ on θ, Δ, and θ' for $V_\infty = 2.5$ m/s, $\phi_\infty = 70\%$, and $T_{fb} = 275$ K

against X in Figure 4(b). For a given value of relative humidity, the rise of T_∞ is accompanied by an increase in the absolute moisture content of the humid air. This increase causes an enhanced potential for vapor diffusion, resulting in a greater number of molecules being condensed at the interface. Consequently, the condensate film becomes thicker.

The value of the fin temperature gradient θ' is also calculated, to indicate the extent to which the rate of heat transfer from the fin to its base depends on air temperature. From Figure 4(c), it is seen that as T_∞ increases, the values of θ' for a given value of X become smaller, resulting in an enhanced rate of heat transfer from the fin to its base.

Taken together, the results of Figure 4 show that increasing T_∞, with all other parameters constant, leads to greater heat and mass transfers from the air to the fin.

The effect of air dry-bulb temperature on heat transfer is shown in Figure 5, the average condensate heat transfer coefficient $\bar{h}_c$ declining as T_∞, due to the thickening of the condensate film. The overall air heat transfer coefficient h_{ov}, however, increases with T_∞. This may be attributed to more intensive heat liberation, associated with condensation. The effect of increasing the temperature difference $T_\infty - T_i$, which might be expected to lead to a fall in the value of h_{ov}, is relatively small.

Figure 5 shows, also, that the calculated fin effectiveness decreases with increasing T_∞. This behavior is explained by Equation 37. With increasing T_∞, the value of the fin parameter N decreases. Hence, the fin effectiveness is reduced in spite of the increase in value of $(-\theta')_0$. As T_∞ varies from 298 K to 323 K, the fin effectiveness falls by about 15%.

Air velocity

Numerical predictions for the variation of θ, Δ, and θ' with X at various air velocities were made and were found to take the same form as Figure 4. An increase in air velocity resulted in lower values of both θ and θ', and higher values of Δ at a given X.[9] These effects are attributed to the increase in the air side heat transfer coefficient and mass transfer coefficient, caused by the increased air flow velocity.

In Figure 6, as the air velocity increases, $\bar{h}_c$ falls. However, the wet fin effectiveness η_w is seen to reduce with increased air velocity. This fall is associated with the increase in the overall air side transfer coefficient, h_{ov}, calculated from the laminar boundary layer equations for air. Thus, the value of the fin parameter N in Equation 37 is reduced and, with it, the wet fin effectiveness η_w. In the determination of h_{ov}, the effect of natural convection has been ignored. It may be readily shown that such effects are of negligible importance, except possibly when the lowest air velocity (V_∞) occurs with the greatest temperature difference ($T_\infty - T_{fb}$).

Air relative humidity

For a given value of X, increasing air relative humidities lead to steady reductions in θ and θ' and to a gradual increase in Δ, the forms of these variations being similar to those exhibited in Figure 4.[9] The total heat removed during cooling and dehumidifying processes is expressed by Equation 7 as the sum of the sensible heat and latent heat. The sensible heat is only slightly affected by relative humidity variations. However, the latent heat contribution increases with higher ϕ_∞, since it is proportional to the difference in moisture content of the air at bulk and interface conditions. Hence, an enhanced rate of heat transfer towards the fin results, leading to a fall in the computed values of θ and θ' and to greater values of Δ.

Distributions of $\bar{h}_c$, η_w, and h_{ov} against ϕ_∞ are shown in Figure 7. There is a steady decline in $\bar{h}_c$ as ϕ_∞ increases, while

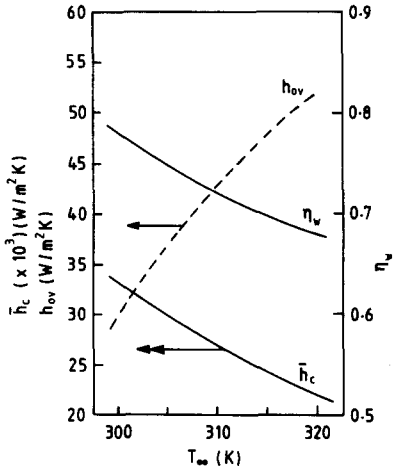

Figure 5 Effect of T_∞ on $\bar{h}_c$, h_{ov}, and η_w for $V_\infty = 2.5$ m/s, $\phi_\infty = 70\%$, $T_{fb} = 275$ K

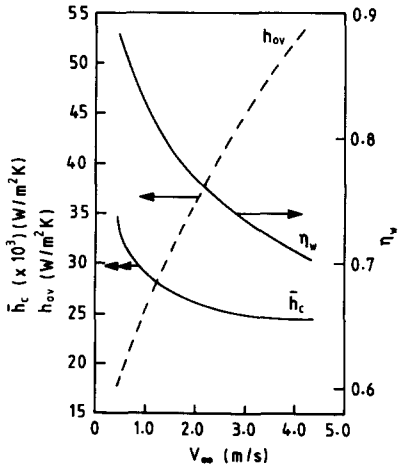

Figure 6 Effect of V_∞ on $\bar{h}_c$, h_{ov}, and η_w for $T_\infty = 308$ K, $\phi_\infty = 70\%$, $T_{fb} = 275$ K

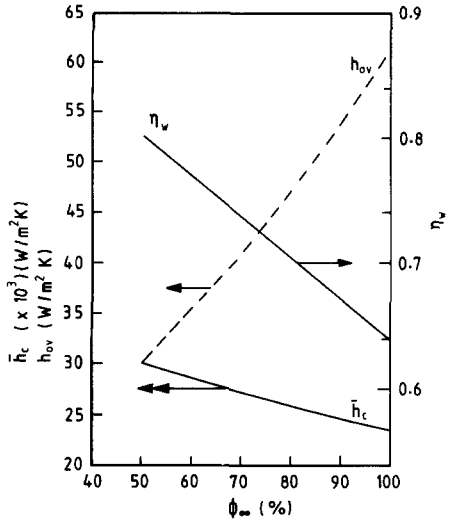

Figure 7 Effect of ϕ_∞ on $\bar{h}_c$, h_{ov}, and η_w for $V_\infty = 2.5$ m/s, $T_\infty = 308$ K, $T_{fb} = 275$ K

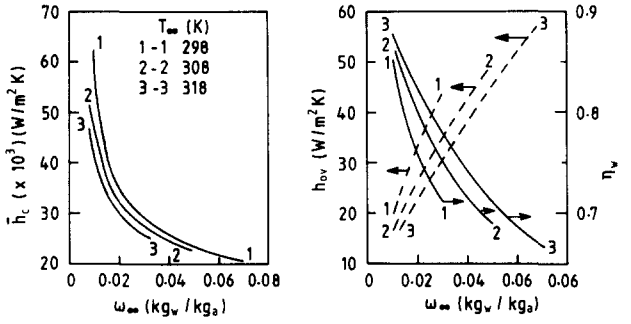

Figure 8 Effect of ω_∞ on $\bar{h}_c$, h_{ov}, and η_w for $V_\infty = 2.5$ m/s, $T_{fb} = 275$ K and three values of T_∞

because of lowered sensible heat factor, h_{ov} increases. In consequence, the value of the fin parameter N falls and with it wet fin effectiveness, η_w.

Air moisture content

In Figure 8 the influence of varying air moisture content on the heat transfer is shown for a range of air dry-bulb temperatures. For a given air velocity and dry-bulb temperature, an increase in moisture content raises the potential for vapor diffusion. This increase results in an enhanced rate of condensation and, consequently, a thicker condensate film, causing a marked reduction in $\bar{h}_c$. However, the value of h_{ov} increases, due to the greater latent heat liberation resulting from phase change, hence reducing η_w.

At a constant moisture content, an increase in T_∞ causes a reduction in the moisture condensed on the fin surface. Because of this, the condensate film thickness becomes thinner, giving a rise in $\bar{h}_c$. At the same time, the ratio of latent heat to total heat becomes smaller due to an increased temperature difference between the bulk air and its dew point. This results in a higher η_w and a lower h_{ov}.

When $\bar{h}_c$, h_{ov}, and η_w were plotted against ω_∞, for various constant values of V_∞ but with T_∞ and T_{fb} fixed, the variations followed trends similar to those shown in Figure 8;[9] the implication is that the heat and mass transfers are controlled by the aerodynamics. For a given value of ω_∞, $\bar{h}_c$, and η_w fall, while h_{ov} becomes greater with increase in V_∞. The computed values for h_{ov} agree with the results of Lebedev *et al.*[13]

The variations of θ, Δ, and θ' with X for a variety of fin base temperatures were calculated. It was foun that the results took the form of those shown in Figure 4, but were little affected by the variation in fin base temperature, as were heat transfer parameters.[9]

Conclusions

In the present study, the performance of a cooled longitudinal fin, in a moist airflow was investigated theoretically. The numerical investigation primarily involved solution of the governing equations to determine fin temperature distribution, condensate film thickness and heat transfer parameters for a range of humid air conditions in the laminar airflow regime. A solution for the vertical longitudinal fin temperature distribution, together with the condensate film thickness distribution in the wet case, has emerged.

(1) The dry effectiveness is dependent only on the air-side heat transfer coefficient.
(2) The rates of heat and mass transfer toward the cooled fin surface, as expressed by the variations in the dimensionless fin temperature, condensate film thickness and fin temperature gradient, are affected significantly by the airflow.
(3) In the presence of condensation, the fin effectiveness decreases, its reduction being a function of the additional thermal resistance associated with the condensate layer. This effect is greatly influenced by the airflow parameters.
(4) The overall heat transfer coefficient is dependent on the fin aerodynamics and is significantly affected by the ratio of sensible to total heat, which is dependent on humid air properties.

Appendix

The subroutine used is D02HBF from the NAG FORTRAN Library Routine Document; D02 Ordinary Differential Equations.

This subroutine solves the two-point boundary value problem, using initial value technique (D02PAF) and Newton iteration.

Initially, Equation 26 is a second-order ordinary differential equation. Therefore, it is reduced to two first-order equations. Hence, three first-order equations are obtained as follows:

$$\frac{d\theta}{dX} = W \tag{A1}$$

$$\frac{d\Delta}{dX} = \frac{\theta}{J(R\Delta^2 + \Delta^3)} \tag{A2}$$

$$\frac{dW}{dX} = \frac{S\theta}{\Delta + N} \tag{A3}$$

These variables θ, Δ, and W, are then renamed as

$$\theta = Y(1),\ \Delta = Y(2),\ \text{and}\ W = Y(3). \tag{A4}$$

Therefore, the above equations can be written as

$$F(1) = \frac{dY(1)}{dX} = Y(3) \tag{A5}$$

$$F(2) = \frac{dY(2)}{dX} = \frac{Y(1)}{J[RY(2)^3 + Y(2)^2]} \tag{A6}$$

$$F(3)=\frac{dY(3)}{dX}=\frac{SY(1)}{Y(2)+N} \quad \text{(A7)}$$

Since two boundary conditions at the initial point ($X=0$) are specified ((1)=1.0, (0)=0.0), only one parameter is needed, the value of which will be estimated for the first iteration, i.e.,

PARAM(1)=$Y(3)$ at $X=0.0$

This estimated value is corrected by a Newton iteration. The Newton correction on each iteration is calculated using a Jacobian matrix whose (i, j)th element depends on the derivative of the ith component of the solution; Y_i with respect to the jth parameter; $P(J)$. This matrix is calculated by a simple numerical differentiation technique which requires N1 integration of the differential system.

References

1 Goodman, W. Dehumidification of air with coils. *Refrig. Engng.* 1936, **32**, 225

2 Goodman, W. Performance of coils for dehumidifying air. *Heating, Piping and Air Conditioning* 1938, **10**, 697ff

3 Tuve, G. L. and Seigel, L. G. Performance of surface-coil dehumidifiers for comfort air conditioning. *Trans. ASHRAE* 1938, **44**, 523ff

4 Threlkeld, J. L. *Thermal Environmental Engineering*, 2nd ed., Prentice-Hall, Englewood Cliffs, New Jersey, 1970

5 ARI Standard 410-72, Forced circulation air-cooling and air-heating coils. Air Conditioning and Refrigeration Institute, 1972

6 Ware, C. D. and Hacha, T. H. Heat transfer from humid air to fin and tube extended surface cooling coils. ASME paper No. 60-HT-17, 1960

7 McQuiston, F. C. Fin efficiency with combined heat and mass transfer. *Trans. ASHRAE* 1973, **81**(1), 350–355

8 Kilic, A. and Onat, K. The optimum shape for convecting rectangular fins when condensation occurs. *Warme- und Stoffübertragung* 1981, **15**, 125–133

9 El-Shafei, E. A. M. Performance of a longitudinal fin with and without condensation from humid air. Ph.D. Thesis, Leeds University, 1986

10 Butterworth, D. and Hewitt, G. F. *Two-phase Flow and Heat Transfer*. Oxford University Press, 1977, 394–442

11 Rogers, G. F. C. and Mayhew, Y. T. *Thermodynamic and Transport Properties of Fluids*, 2nd ed. S.I. Units, 1969

12 Sparrow, E. M. and Gregg, J. L. A boundary layer treatment of laminar-film condensation. *Trans. ASME*, 1959, **81**, 13–18

13 Lebedev, P. D., Baklascov, A. M., and Sergazin, Zh. F. Aerodynamics, heat and mass transfer in vapour condensation from humid air on a flat plate in a longitudinal flow in a symmetrically cooled slot. *Ont. J. Heat Mass Transfer* 1969, **12**, 833–842